

# Influence of $\gamma$ -radiation on the reactivity of montmorillonite towards $\text{H}_2\text{O}_2$

Michael Holmboe\*, Mats Jonsson and  
Susanna Wold

*KTH Chemical Science and Engineering*

Nuclear Chemistry  
Royal Institute of Technology  
SE-100 44 Stockholm, Sweden

\*Corresponding author. Fax: +46 8 7908772.

E-mail: holmboe@kth.se (M. Holmboe)

## Abstract

Compacted and water saturated bentonite will be used as an engineered barrier in deep geological repositories for radioactive waste in many countries. Due to the high dose rate of ionizing radiation outside the canisters holding the nuclear waste, radiolysis of the interlayer and pore water in the compacted bentonite is unavoidable. Upon reaction with the oxidizing and reducing species formed by water radiolysis ( $\text{OH}^\bullet$ ,  $e^-_{(\text{aq})}$ ,  $\text{H}^\bullet$ ,  $\text{H}_2\text{O}_2$ ,  $\text{H}_2$ ,  $\text{HO}_2^\bullet$ ,  $\text{H}_3\text{O}^+$ ), the overall redox properties in the bentonite barrier may change. In this study the influence of  $\gamma$ -radiation on the structural Fe(II)/Fe(III) content in montmorillonite and its reactivity towards hydrogen peroxide ( $\text{H}_2\text{O}_2$ ) was investigated in parallel experiments. The results show that under anoxic conditions the structural Fe(II)/Fe<sub>tot</sub> ratio of dispersed montmorillonite are increased from  $\leq 3$  to 25-30% after  $\gamma$ -doses comparable to repository conditions. Furthermore, a strong correlation between the structural Fe(II)/Fe<sub>tot</sub> ratio and the  $\text{H}_2\text{O}_2$  decomposition rate in montmorillonite dispersions was found. This correlation was further verified in experiments with consecutive  $\text{H}_2\text{O}_2$  additions, since the structural Fe(II)/Fe<sub>tot</sub> ratio was seen to decrease concordantly. This work shows that the structural iron in montmorillonite could be a sink for one of the major oxidants formed upon water radiolysis in the bentonite barrier,  $\text{H}_2\text{O}_2$ .

## 1. Introduction

Deep geological repositories for spent nuclear fuel consist of several natural and engineered barriers to prevent groundwater intrusion and radionuclide transport. According to the KBS-3 concept, which will be used in Sweden and Finland, the spent nuclear fuel will be placed in cast iron canisters covered by copper. The canisters will be placed approximately 500 m below ground in the granite bedrock. In the cylindrical holes made for

the canisters in the bedrock, bentonite clay will be used as a buffer material between the canister and the bedrock. At the time when the canisters are placed in the repository, the dose rate at the interface between the copper and bentonite is expected to be 0.1-0.5 Gy h<sup>-1</sup> [1]. Hence, even when none of the barriers fail, the clay buffer will be exposed to ionizing radiation. The effects of ionizing radiation on the barrier integrity of bentonite must therefore be elucidated to be incorporated in the safety assessment. The effects could be both direct (energy absorbed by the clay) and indirect (energy absorbed by pore water). The aqueous radiolysis products can affect the redox properties not only of the bentonite barrier itself but also in the immediate environment. Hydrogen peroxide ( $\text{H}_2\text{O}_2$ ) has been identified as one of the major oxidants formed by water radiolysis and as such its reactivity must be investigated. In a recent study we found that ionizing radiation increases the stability of montmorillonite colloids [2]. An increase in the Fe(II)/Fe(III) ratio which intuitively would increase the negative surface charge of montmorillonite were discussed as one of the possible reasons. However this could not be supported by the experimental results. As for the saturated bentonite itself, very few attempts have been made to understand the fate of the structural Fe(II)/Fe(III) ratio and overall impact of water radiolysis under  $\gamma$ -irradiation. Thus, this study is devoted to the understanding of the effect of  $\gamma$ -irradiation under anoxic conditions on the structural Fe(II)/Fe(III) ratio of the main component of bentonite, montmorillonite, as well as its overall reactivity towards  $\text{H}_2\text{O}_2$ .

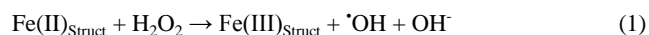
Montmorillonite, which is a smectite mineral, is made up of an aluminum octahedral sheet sandwiched between two silica tetrahedral sheets into individual layer particles, with the dimensions of approx. 0.95 nm in height and several hundred nm in the lateral dimensions. The montmorillonite particles may contain iron as *i*) structural Fe (usually substituting aluminum in the octahedral sheet) *ii*) Fe-oxides sorbed onto the layer surface; *iii*) Fe ions complexed by surface hydroxyl groups on the edge of the montmorillonite layer. A typical native bentonite, such as the widely studied Wyoming Bentonite MX-80, consists of nearly 3 wt% Fe, the major part being structural Fe(III) replacing Al<sup>3+</sup> in the aluminum octahedral sheet [3]. At elevated Fe(II)/Fe<sub>tot</sub> ratios however, significant changes in several physical properties such as the swelling pressure, cation exchange capacity (CEC), total layer charge, specific surface area as well as microstructural properties has been found in previous studies [4-9].

After the initial saturation of the bentonite barrier, anoxic conditions are expected. Furthermore, during its initial lifetime, the bentonite barrier adjacent to the canister surface will be subjected to approx. 40-200 kGy of mainly  $\gamma$ -radiation from Cs-137 (t<sub>1/2</sub> 30.1 yrs), calculated from the initial dose rate reported in [1]. The effect of the ionizing radiation on the bulk physical properties of the bentonite barrier, such as swelling pressure and hydraulic conductivity, is expected to be small [10]. Apart from reacting with the actual montmorillonite, the primary oxidizing and reducing species formed upon water radiolysis ( $\text{OH}^\bullet$ ,  $e^-_{(\text{aq})}$ ,

H<sup>+</sup>, H<sub>2</sub>O<sub>2</sub>, H<sub>2</sub>, HO<sub>2</sub><sup>•</sup>, H<sub>3</sub>O<sup>+</sup>) can react with the solute species in pore- and interlayers voids. Because of this, the structural Fe(II)/Fe(III) ratio in montmorillonite and overall redox properties in the bentonite barrier may change, which may also affect the immediate environment such as the copper canister holding the nuclear waste. In the past, effects like H<sub>2</sub> and the H<sub>2</sub>O<sub>2</sub> production in clay systems were mainly studied, as dependent on groundwater or the pore water composition in bentonite. Eriksen et al. [11-13] investigated both bentonite and groundwater submitted to  $\alpha$ ,  $\beta$  and  $\gamma$ -irradiation and concluded that the overall H<sub>2</sub> and H<sub>2</sub>O<sub>2</sub> production ultimately depend on the available dissolved solutes, such as Fe<sup>2+</sup> and HCO<sub>3</sub><sup>-</sup>, as well as the type of radiation, due to their different LET (Linear Energy Transfer) values.

Fattahi et al. [14] investigated the H<sub>2</sub>O<sub>2</sub> production and decomposition in oxygenated clay water as a function of  $\gamma$ -irradiation. It was found that the radiation chemical yield, (G-value) for H<sub>2</sub>O<sub>2</sub> production in the oxygenated clay supernatant was approx. twice (0.25  $\mu$ mol/J) the yield in pure water.

It is well known that the  $\cdot$ OH and e<sup>-</sup><sub>(aq)</sub> radicals react with most chemical species with very high rate constants. As for H<sub>2</sub>O<sub>2</sub> many of its reactions are relatively slow but can easily be catalyzed by redox active impurities such as Fe(II)/Fe(III) ions. In general, the decomposition of H<sub>2</sub>O<sub>2</sub> is often accompanied by the generation of highly reactive oxygen species. In earlier studies the Fenton reaction have been shown to be a major decomposition route for H<sub>2</sub>O<sub>2</sub>, through oxidation of Fe(II) to Fe(III).



Thus, it is likely that an increase in the structural Fe(II)/Fe(III) ratio in montmorillonite significantly could influence the decomposition of H<sub>2</sub>O<sub>2</sub>. The purpose of this study was hence to investigate the reactivity of  $\gamma$ -irradiated montmorillonite dispersions towards H<sub>2</sub>O<sub>2</sub> by monitoring the [H<sub>2</sub>O<sub>2</sub>]<sub>t</sub>/[H<sub>2</sub>O<sub>2</sub>]<sub>0</sub> ratio with time, as well as to determine the structural Fe(II)/Fe<sub>Tot</sub> ratio in parallel experiments.

## 2. Experimental section

### 2.1 Materials

Chemicals: Hydrogen peroxide, H<sub>2</sub>O<sub>2</sub> (30 wt%), Sodium Citrate (Na<sub>3</sub>Cit), Sodium bicarbonate (NaHCO<sub>3</sub>) Sodium sulfate (Na<sub>2</sub>SO<sub>4</sub>), sulfuric acid (H<sub>2</sub>SO<sub>4</sub>), Potassium Chloride (KI), Sodium acetate, (NaAc) were of puriss p.a. or comparable grade. ADM solution containing 3wt% (NH<sub>4</sub>)<sub>2</sub>Mo<sub>2</sub>O<sub>7</sub>.

Clay mineral: In this study the Wyoming Swy-2 montmorillonite reference clay from the Clay Mineral society, hereafter denoted as WyNa, was used. For reproducibility reasons some experiments required a purified Na-montmorillonite (denoted WyNa<sub>w</sub>) which was obtained by the following pretreatment: 1) Sodium exchange was facilitated by washing and centrifugation three times using a 0.5 M Na<sub>2</sub>SO<sub>4</sub> solution, keeping only the smectite portion after each centrifugation cycle. 2) Free iron oxides were removed by a CB (Citrate-Bicarbonate) method. In short, approximately 50 g of clay was dispersed and stirred under heating

(70 °C) for 6 hours in 1 L of 0.1 M Na<sub>3</sub>Cit in a 0.3 M NaHCO<sub>3</sub> buffer. The obtained sample was then washed three times in a 0.1 M Na<sub>2</sub>SO<sub>4</sub> solution, keeping only the smectite portion after each centrifugation cycle. 3) Organic residues and remaining citrate was removed by stirring the resulting suspension in 2 M H<sub>2</sub>O<sub>2</sub> at 70 °C for 6 hours. 4) In order to remove excess carbonate the suspension was stirred at 70 °C at pH 1 after addition of H<sub>2</sub>SO<sub>4</sub> for 6 hours. Finally the pH of the suspension was neutralized by addition of small aliquots of NaOH. The remaining dispersion was then dried at 120 °C and grinded to a fine powder. All dispersions of the different clay types used (WyNa/WyNa<sub>w</sub>), were prepared from 2 wt% stock solutions, prepared at least one day prior the experiments.

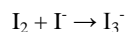
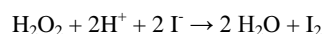
## 2.2 Methods

### 2.2.1 $\gamma$ -irradiations

The  $\gamma$ -irradiations were conducted using a Gammacell 1000 Elite <sup>137</sup>Cs-source, with a dose rate of 0.15 Gy/s or 13 kGy/day (as determined by Fricke dosimetry). Samples irradiated under anoxic conditions were degassed with N<sub>2</sub> for a minimum of 30 min. In one set of experiments in order to achieve strictly reducing conditions, 5 % isopropanol were added [15].

### 2.2.2 H<sub>2</sub>O<sub>2</sub> determination

After filtrating the montmorillonite dispersions with a 0.45  $\mu$ m syringe filter, the solution concentration of H<sub>2</sub>O<sub>2</sub> was analyzed indirectly by a spectroscopic method by observing the I<sub>3</sub><sup>-</sup> concentration at 360 nm [16-18]. The overall reaction proceeds through reaction 1 and 2.



In detail, 0.5 mL of a sample filtrate was analyzed by addition of 0.100  $\mu$ L of freshly prepared 1 M KI, 0.100  $\mu$ L HAc/NaAc buffer (containing a few drops of the ADM solution) in a total volume of 2 mL. The subsequent I<sub>3</sub><sup>-</sup> concentration was measured at 360 nm with a JASCO V-630 UV/Vis spectrophotometer.

### 2.2.3 Structural Fe(II)/Fe(III) determination

The structural Fe(II)/Fe(III) was analyzed using the 1,10-phenanthroline (phen) method described by Amonette and Templeton [19]. In this spectroscopic method the structural Fe(II) can be analyzed after complete acid digestion by measuring the adsorption of the red Fe(II)-phen complex at 510 nm. Since the Fe(III)-phen complex is colorless, the total structural Fe and structural Fe(III) concentrations are obtained after complete reduction by hydroxylamine. In detail, 40 mg of montmorillonite, either dispersed or in powder form, was added to a nearly boiling acid mixture consisting of 1:2:12 mL of HF (48wt%):phen (10wt% in EtOH): H<sub>2</sub>SO<sub>4</sub> (10wt%). After boiling for 30 min and complete digestion, 10 mL of H<sub>3</sub>BO<sub>3</sub> (5wt%) and 90 mL of water was added to ensure long term stability of the resulting digestate. In the structural Fe(II) determination, 1 mL of the digestate was diluted with 10 mL of Na<sub>3</sub>Cit (1wt%) and measured at 510 nm. In

the structural  $\text{Fe}_{\text{Tot}}$  and hence the structural Fe(III) determination, the digestate was first let to react for at least 120 min in 10 mL of  $\text{Na}_3\text{Cit}$  (1wt%) also containing 1 wt%  $\text{NH}_3\text{OHCl}$ , before measurement of the absorption.

### 3. Results and discussion

#### 3.1 $\text{H}_2\text{O}_2$ decomposition on different pre-treated clays

It was initially discovered that the  $\text{H}_2\text{O}_2$  decomposition rate in untreated WyNa dispersions was slow but not negligible. In figure 1a-c, the  $\text{H}_2\text{O}_2$  decomposition during 24 hours is shown in the different unirradiated clay dispersions used in this study. As can be seen in figure 1a, the overall decomposition rate in the untreated WyNa dispersions is not negligible.

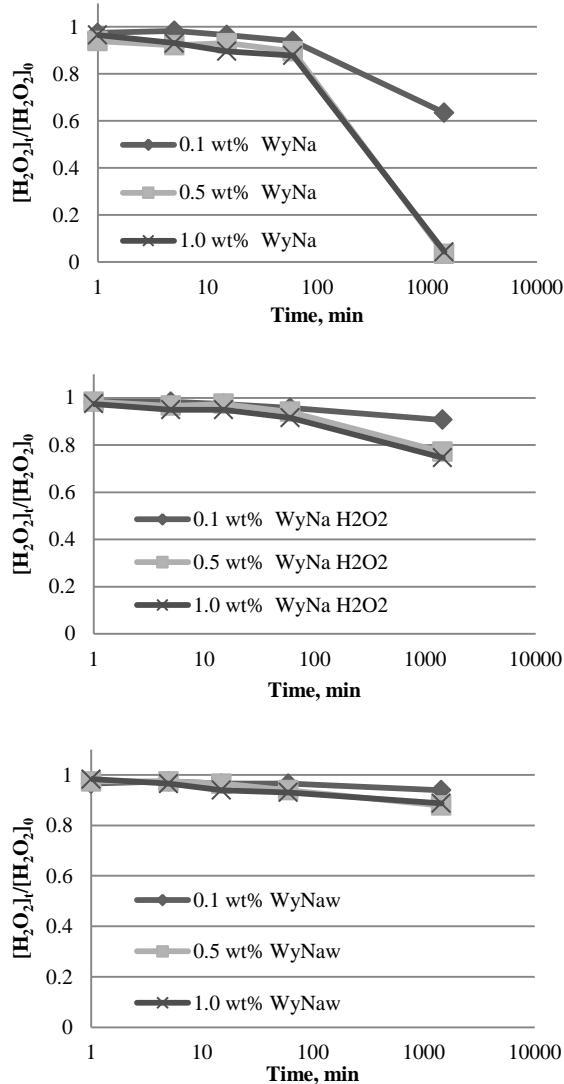


**Figure 1.**  $\text{H}_2\text{O}_2$  decomposition rates in different clay dispersions. a) WyNa b) WyNa after  $\text{H}_2\text{O}_2$  pre-treatment c) WyNa<sub>w</sub>.

For the two highest concentrations used, no  $\text{H}_2\text{O}_2$  was found after 24 h, likely due to reaction with soluble Fe(II)/Fe(III) species, Fe-oxides or traces of organics in the clay. Figure 1b displays the  $\text{H}_2\text{O}_2$  decomposition in a WyNa clay treated with  $\text{H}_2\text{O}_2$  (step 3 in section 2.1) prior the experiment. Compared to the untreated WyNa, a significantly lower decomposition rate of  $\text{H}_2\text{O}_2$  was found, indicating increased  $\text{H}_2\text{O}_2$  stability after the  $\text{H}_2\text{O}_2$  pre-treatment. In the WyNa<sub>w</sub> dispersions however, the  $\text{H}_2\text{O}_2$  stability was found to be even higher, with a decomposition rate of approx. 10% in 24 h. A possible explanation to this trend could be found in the corresponding Fe(II)/Fe(III) ratio in the different clay types. Prior this investigation the total Fe content of the WyNa clay was found to be  $2.9 \pm 0.05$  wt% ( $n=5$ ) with a structural Fe(II)/Fe<sub>Tot</sub> ratio of 3% using the method of [19]. The  $\text{H}_2\text{O}_2$  pre-treatment was unexpectedly not found to alter the overall the Fe(II) content significantly. For the WyNa<sub>w</sub> clay however, a small decrease in the total Fe content and in the structural Fe(II)/Fe<sub>Tot</sub> ratio was found,  $2.7 \pm 0.1$  wt% ( $n=6$ ), and 1.7%, respectively. This indicates that free Fe-oxides and soluble Fe species that were removed from the WyNa<sub>w</sub> clay contribute to the  $\text{H}_2\text{O}_2$  decomposition. The decrease in the  $\text{H}_2\text{O}_2$  decomposition rates between the as received WyNa clay compared to the  $\text{H}_2\text{O}_2$  pre-treated clay can be explained by the absence of organic matter in the latter. This is because organic matter could uphold catalytic cycling of Fe(II)/Fe(III) if a reducing organic radical is formed by reacting with the  $\text{OH}^\bullet$  radical formed in reaction 1.

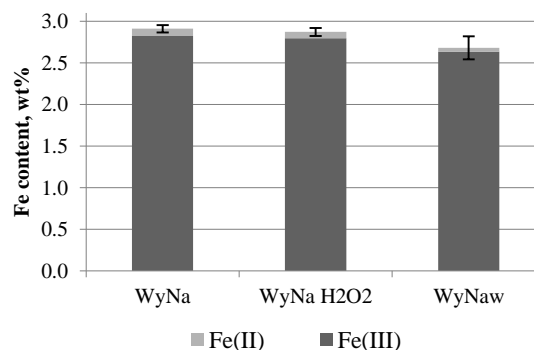


**Figure 2.** Fe(II)/Fe(III) content in the different clay types used in this study under ambient conditions.

#### 3.2 $\gamma$ -irradiation under anoxic conditions

The effect of  $\gamma$ -irradiation under anoxic conditions on the reactivity of WyNa<sub>w</sub> dispersions towards  $\text{H}_2\text{O}_2$  can be seen in figures 3a-e. The dispersions were irradiated for 1, 3, 6, 12 and 24 hours, corresponding to 0.54; 1.62; 3.2; 6.5; 13.0 kGy. After 1 h of  $\gamma$ -irradiation no significant decomposition of  $\text{H}_2\text{O}_2$  was found compared to the corresponding unirradiated dispersions shown in figure 1c. However, after 3 hours of irradiation a substantial decomposition was observed, increasing with increasing clay concentration. This trend with increasing decomposition rate with increasing irradiation time and clay concentration was also seen

in the 6 h; 12h; and 24 h experiments, figure 3c-e, although the relative increase in observed decomposition rates with increasing irradiation time, seemed to decrease after 6 h of irradiation. In order to investigate the contribution of the  $\text{H}_2\text{O}_2$  decomposition in the solution phase after  $\gamma$ -irradiation, the  $\text{H}_2\text{O}_2$  decomposition in a centrifuged supernatant from a 24 h sample was also measured, shown in figure 3f. In the supernatant samples a small increased

decomposition rate was found compared to the unirradiated equivalents suggesting increased montmorillonite dissolution upon  $\gamma$ -irradiation. However, compared to the  $\text{H}_2\text{O}_2$  decomposition rates of the  $\gamma$ -irradiated  $\text{WyNa}_w$  dispersions, this effect is small. The corresponding  $\text{Fe(II)}/\text{Fe(III)}$  contents in 0.4 wt%  $\gamma$ -irradiated  $\text{WyNa}_w$  dispersions is displayed in figure 4.

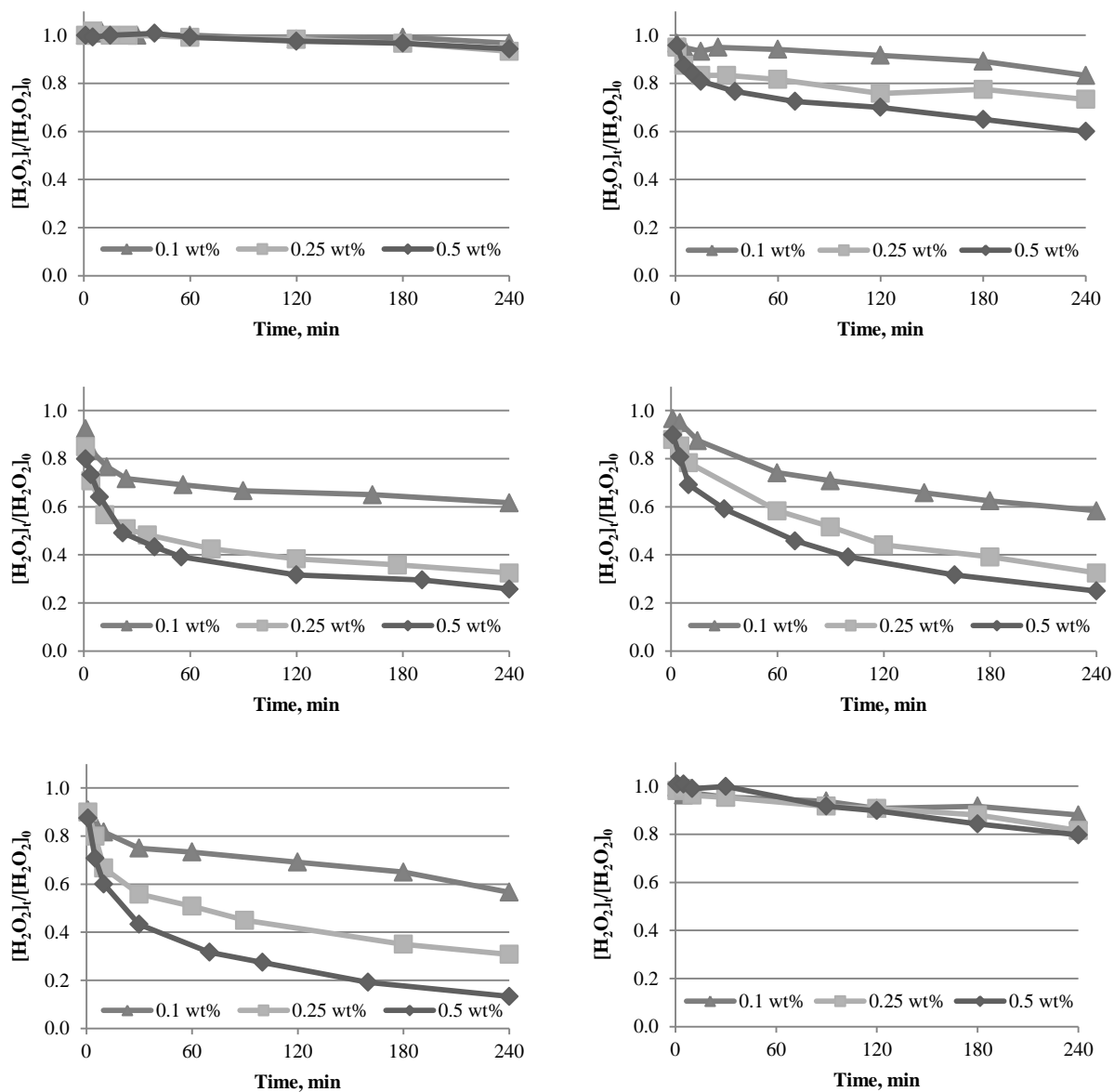


**Figure 3.**  $\text{H}_2\text{O}_2$  decomposition rates in  $\text{WyNa}_w$  dispersions irradiated a) 1 h b) 3 h c) 6 h d) 12 h e) 24 h f) 24 h, only supernatant.

Except the small decrease in the structural Fe(II) content from the 12 h to the 24 h sample, with increasing dose a general increase in the structural Fe(II) content was observed, supporting the findings of increasing  $\text{H}_2\text{O}_2$  decomposition rates with increasing irradiation dose. In order to control the effect of  $\text{H}_2\text{O}_2$  on the structural Fe(II)/Fe<sub>Tot</sub> ratio, an addition of 0.2 mM  $\text{H}_2\text{O}_2$  was also made resulting in an apparent decrease in the structural Fe(II)/Fe<sub>Tot</sub> ratio. This general increase in the structural Fe(II)/Fe<sub>Tot</sub> ratio can be explained by the fact that the initial reduction rate of structural Fe(III) by the  $e^-_{(aq)}$  radical would be higher than the corresponding oxidation rate of the structural Fe(II) by the  $\cdot\text{OH}$  radical, if the  $\cdot\text{OH}$  and  $e^-_{(aq)}$  radicals would react with similar rate constants, since under ambient conditions the structural Fe(II)/Fe(III) ratio is very low,  $\leq 5\%$ . In order to relate these results to our previous findings in [2] regarding increased colloid stability upon  $\gamma$ -irradiation, a settling experiment with  $\gamma$ -irradiated and unirradiated 0.2 wt% WyNa<sub>w</sub> dispersions was performed (not shown). After irradiation for 24 h, 15 mM NaCl was added to induce colloid aggregation and rapid settling. Compared to the unirradiated reference, irradiated WyNa<sub>w</sub> dispersions displayed significantly slower settling rates, regardless of the samples were irradiated under anoxic or oxic conditions, or if 2 mM  $\text{H}_2\text{O}_2$  was added to the dispersion (prior NaCl). Since both  $\text{H}_2\text{O}_2$  and irradiation under oxic conditions suppresses the structural Fe(II) content in montmorillonite, these results indicate that the structural Fe(II)/Fe(III) ratio do not influence the colloid stability significantly.

### 3.3 $\gamma$ -irradiation under reducing conditions

In order to investigate the effect of  $\text{H}_2\text{O}_2$  additions on the elevated structural Fe(II)<sub>Struct</sub>/Fe<sub>Tot</sub> ratios,  $\gamma$ -irradiations under strictly reducing conditions was also performed. This was accomplished using 0.4 wt% WyNa<sub>w</sub> dispersions with 5 v% isopropanol, since this additive effectively scavenges the main transient oxidant formed upon water radiolysis, i.e. the  $\cdot\text{OH}$  radical, while itself forming a reducing  $\alpha$ -hydroxyl-alkyl radical [15]. The resulting Fe(II)<sub>Struct</sub>/Fe<sub>Tot</sub> ratios at different  $\gamma$ -radiation doses are displayed in figure 5. As can be seen, an incomparable decrease with irradiation time was observed. After 24 hours of irradiation the structural Fe(II)/Fe<sub>Tot</sub> ratio reached 0.85, significantly exceeding the maximum Fe(II)<sub>Struct</sub>/Fe<sub>Tot</sub> ratio obtained from the  $\gamma$ -irradiations under anoxic conditions. For the same sample, the effect of consecutive  $\text{H}_2\text{O}_2$  additions is shown in the six outermost columns (to the right) in figure 5, which display the Fe(II)/Fe(III) contents after additions corresponding to 0.2-0.4 mM. Figure 6 show the corresponding  $\text{H}_2\text{O}_2$  decomposition rates, decreasing with increasing amount of added  $\text{H}_2\text{O}_2$ . The arrows in figure 6 indicate sampling points for the Fe(II)/Fe(III) determination, shown in figure 5. Although the decomposition of  $\text{H}_2\text{O}_2$  clearly was dependent on the Fe(II)/Fe<sub>Tot</sub> ratio, the Fenton reaction (reaction 1) cannot be the only route for  $\text{H}_2\text{O}_2$  decomposition in the irradiated clay dispersions. This is because the effective/accumulated Fe(II) concentration (taking the repeated dilutions from the  $\text{H}_2\text{O}_2$  additions into account) in the WyNa<sub>w</sub> dispersion was significantly lower than the total accumulated addition of  $\text{H}_2\text{O}_2$  (1.3 mmoles/L and 2.0 mmoles/L, respectively).

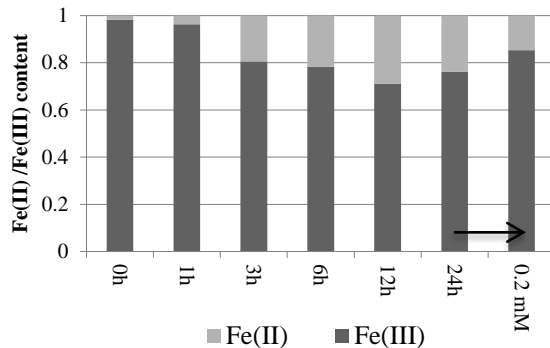


**Figure 4.** Normalized Fe(II)/Fe(III) contents in the WyNa<sub>w</sub> dispersions after  $\gamma$ -irradiation. The outermost columns (to the right) display the Fe(II)/Fe(III) content after  $\text{H}_2\text{O}_2$  addition to the 24 h sample.

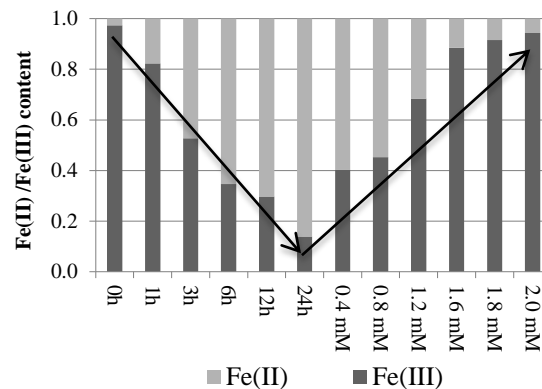


**Figure 5.** Normalized Fe(II)/Fe(III) contents in the WyNa<sub>w</sub> dispersions after  $\gamma$ -irradiation under strictly reducing conditions. The six outermost columns (to the right) display the Fe(II)/Fe(III) contents after consecutive  $\text{H}_2\text{O}_2$  additions to the 24 h sample.

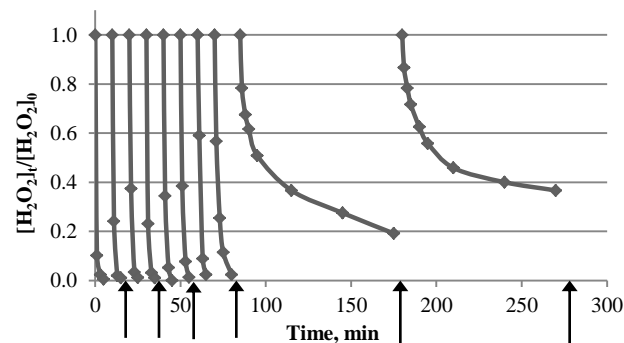


**Figure 6.** Decomposition of  $\text{H}_2\text{O}_2$  after consecutive additions of 0.2 mM to WyNa<sub>w</sub>, irradiated for 24 h under strictly reducing conditions. Arrows indicate sampling for the Fe(II)/Fe(III) determinations in Figure 5.

#### 4. Conclusions

This study examined the structural Fe(II)/Fe<sub>Tot</sub> ratio in montmorillonite and its reactivity towards H<sub>2</sub>O<sub>2</sub> in parallel experiments, as a function of  $\gamma$ -dose. Prior irradiation, the Fe(II)/Fe<sub>Tot</sub> ratio in the studied clay (WyNa<sub>w</sub>) was < 3 % out of a total Fe content of 2.7±0.10 wt% and the H<sub>2</sub>O<sub>2</sub> decomposition rate low. However, much higher structural Fe(II)/Fe<sub>Tot</sub> ratios, approx. 25-30%, was found after  $\gamma$ -irradiation under anoxic conditions, resulting in substantially higher H<sub>2</sub>O<sub>2</sub> decomposition rates. This effect can be explained by a higher production rate of structural Fe(II) over Fe(III), due to the low initial Fe(II)/Fe<sub>Tot</sub> ratio, assuming similar reaction rates with the transient reductants and oxidants formed upon water radiolysis, (mainly e<sup>-</sup><sub>(aq)</sub> and OH<sup>•</sup>, respectively). However, this elevated structural Fe(II)/Fe<sub>Tot</sub> ratio could not explain the radiation induced increase in colloid stability of montmorillonite found in [2]. The correlation between the structural Fe(II)/Fe<sub>Tot</sub> ratio and H<sub>2</sub>O<sub>2</sub> decomposition was further verified in experiments where consecutive H<sub>2</sub>O<sub>2</sub> additions was made, since the structural Fe(II)/Fe<sub>Tot</sub> ratio was seen to decrease concordantly. The results from this study strongly implies that  $\gamma$ -radiation may alter the redox properties of the bentonite barrier in a deep geological repository for nuclear waste, accelerating the decomposition of one of the major oxidants formed upon water radiolysis, H<sub>2</sub>O<sub>2</sub>.

#### 6. References

- [1] R. Håkansson, Beräkning av nuklidinnehåll, resteffekt, aktivitet samt doshastighet för utbränt kärnbränsle, in, R-99-74, SKB AB, 1999.
- [2] M. Holmboe, S. Wold, M. Jonsson, S. Garcia-Garcia, Effects of  $\gamma$ -irradiation on the stability of colloidal Na<sup>+</sup>-Montmorillonite dispersions, *Appl. Clay Sci.*, 43 (2009) 86-90.
- [3] O. Karnland, S. Olsson, U. Nilsson, Mineralogy and sealing properties of various bentonites and smectite-rich clay material, SKB AB, Swedish Nuclear Fuel and Waste Management Co., 2006.
- [4] E.M. Khaled, J.W. Stucki, Iron oxidation state effects on cation fixation in smectites, *Soil Sci. Soc. Am. J.*, 55 (1991) 550-554.
- [5] J.W. Stucki, D. Tessier, Effects of iron oxidation state on the texture and structural order of Na-nontronite gels, *Clay. Clay. Miner.*, 39 (1991) 137-143.
- [6] J.W. Stucki, D. Golden, C.B. Roth, Effects of reduction and reoxidation of structural iron on the surface charge and dissolution of dioctahedral smectites, *Clay. Clay. Miner.*, 32 (1984) 350-356.
- [7] P.R. Lear, J.W. Stucki, Intervalence electron transfer and magnetic exchange in reduced nontronite, *Clay. Clay. Miner.*, 35 (1987) 373-378.
- [8] P.R. Lear, J.W. Stucki, Effects of iron oxidation state on the specific surface area of nontronite, *Clay. Clay. Miner.*, 37 (1989) 547-552.
- [9] J.W. Stucki, K. Lee, L. Zhang, R.A. Larson, Effects of iron oxidation state on the surface and structural properties of smectites, *Pure. Appl. Chem.*, 74 (2002) 2145-2158.
- [10] R. Pusch, O. Karnland, A. Lajudie, A. Decarreau, MX 80 clay exposed to high temperatures and gamma radiation, SKB AB, Swedish Nuclear Fuel and Waste Management Co., 1993.
- [11] T. Eriksen, H. Christensen, E. Bjergbakke, Hydrogen production in -irradiated bentonite, *Journal of radioanalytical and nuclear chemistry*, 116 (1987) 13-25.
- [12] T.E. Eriksen, P. Ndalamba, H. Christensen, E. Bjergbakke, Radiolysis of ground water: influence of carbonate and chloride on the hydrogen peroxide production, SKB AB, Swedish Nuclear Fuel and Waste Management Co., 1988.
- [13] T.E. Eriksen, A. Jacobsson, Radiation effects on the chemical environment in a radioactive waste repository, SKB AB, Swedish Nuclear Fuel and Waste Management Co., 1983.
- [14] M. Fattahi, C. Houée-Levin, C. Ferradini, P. Jacquier, Hydrogen peroxide formation and decay in gamma-irradiated clay water, *International Journal of Radiation Applications and Instrumentation. Part C. Radiation Physics and Chemistry*, 40 (1992) 167-173.
- [15] J.W.T. Spinks, R.J. Woods, *An introduction to radiation chemistry*, (1990).
- [16] T.C.J. Ovenston, W.T. Rees, The spectrophotometric determination of small amounts of hydrogen peroxide in aqueous solutions, *Analyst*, 75 (1950) 204-208.
- [17] W.A. Patrick, H.B. Wagner, Determination of hydrogen peroxide in small concentrations, *Analytical Chemistry*, 21 (1949) 1279-1280.
- [18] Y. Nimura, K. Itagaki, K. Nanba, Colorimetric determination of COD (Mn) using hydrogen peroxide, *Nippon Suisan Gakkaishi*, 58 (1992) 1129-1137.
- [19] J.E. Amonette, J.C. Templeton, Improvements to the quantitative assay of nonrefractory minerals for Fe (II) and total Fe using 1, 10-phenanthroline, *Clay. Clay. Miner.*, 46 (1998) 51-62.